Original Research

Improved Aortic Pulse Wave Velocity Assessment From Multislice Two-Directional In-Plane Velocity-Encoded Magnetic Resonance Imaging

Jos J.M. Westenberg, PhD,[1*] Albert de Roos, PhD, MD,[1] Heynric B. Grotenhuis, PhD, MD,[1] Paul Steendijk, PhD,[2] Dennis Hendriksen, MSc,[1] Pieter J. van den Boogaard, BSc,[1] Rob J. van der Geest, MSc,[1] Jeroen J. Bax, PhD, MD,[2] J. Wouter Jukema, PhD, MD,[2] and Johan H.C. Reiber, PhD[1]

Purpose: To evaluate the accuracy and reproducibility of aortic pulse wave velocity (PWV) assessment by in-plane velocity-encoded magnetic resonance imaging (MRI).

Materials and Methods: In 14 patients selected for cardiac catheterization on suspicion of coronary artery disease and 15 healthy volunteers, PWV was assessed with multislice two-directional in-plane velocity-encoded MRI ($PWV_{i.p.}$) and compared with conventionally assessed PWV from multisite one-directional through-plane velocity-encoded MRI ($PWV_{t.p.}$). In patients, PWV was also obtained from intraarterially acquired pressure–time curves ($PWV_{pressure}$), which is considered the gold standard reference method. In volunteers, $PWV_{i.p.}$ and $PWV_{t.p.}$ were obtained in duplicate in the same examination to test reproducibility.

Results: In patients, $PWV_{i.p.}$ showed stronger correlation and similar variation with $PWV_{pressure}$ than $PWV_{t.p.}$ (Pearson correlation $r = 0.75$ vs. $r = 0.58$, and coefficient of variation [COV] = 10% vs. COV = 12%, respectively). In volunteers, repeated $PWV_{i.p.}$ assessment showed stronger correlation and less variation than repeated $PWV_{t.p.}$ (proximal aorta: $r = 0.97$ and COV = 10% vs. $r = 0.69$ and COV = 17%; distal aorta: $r = 0.94$ and COV = 12% vs. $r = 0.90$ and COV = 16%; total aorta: $r = 0.97$ and COV = 7% vs. $r = 0.90$ and COV = 13%).

Conclusion: $PWV_{i.p.}$ is an improvement over conventional $PWV_{t.p.}$ by showing higher agreement as compared to the gold standard ($PWV_{pressure}$) and higher reproducibility for repeated MRI assessment.

Key Words: aorta; compliance; MRI; blood flow; waves; pressure waves
J. Magn. Reson. Imaging 2010;32:1086–1094.

THE AORTIC PULSE WAVE VELOCITY (PWV), defined as the propagation speed of the systolic wave front through the aorta, is a surrogate marker for aortic wall compliance and is considered to be a strong predictor of cardiovascular mortality (1–5). The prognostic value of PWV has been studied in diabetes mellitus (6,7), hypertension (9–13), and Marfan's syndrome (14,15).

PWV assessed from the propagation of pressure waves through the aorta, intraarterially acquired during catheterization with pressure catheters, is considered to be the most accurate and therefore the gold standard reference method (16,17). Tonometry and echo Doppler are established, noninvasive techniques applied for PWV assessment (1–7,9–12,18,19), but both modalities only provide an estimation of the global aortic PWV, due to the limited available acoustic windows along the aorta and the inability to accurately determine the length of the aorta.

Multisite one-directional through-plane velocity-encoded (VE) magnetic resonance imaging (MRI) has been applied for PWV assessment by calculating the speed of the flow wave or the velocity wave propagating through the aorta from the distance between measurement sites and the difference in time (ie, the transit time) of the arrival of the wave front at the respective sites (8,13–15,20–22). The 3D nature of MRI enables an accurate determination of the aortic length without restrictions regarding imaging planes. Grotenhuis et al (22) reported accuracy and reproducibility of multisite one-directional through-plane VE MRI for PWV assessment. Still, considerable variation in PWV assessment between MRI and pressure measurements was reported and correlation with the gold standard was moderate. The purpose of this study was to

[1]Department of Radiology, Leiden University Medical Center, Leiden, The Netherlands.
[2]Department of Cardiology, Leiden University Medical Center, Leiden, The Netherlands.
Contract grant sponsor: Netherlands Heart Foundation; Contract grant number: Project 2006B138; Contract grant sponsor: Dutch Society of Vascular Medicine; Contract grant number: NVVG-MSD 2010 (to A.d.R.).
*Address reprint requests to: J.J.M.W., Leiden University Medical Center, Department of Radiology, Albinusdreef 2, 2333 ZA Leiden, The Netherlands. E-mail: j.j.m.westenberg@lumc.nl
Received May 10, 2010; Accepted August 12, 2010.
DOI 10.1002/jmri.22359
View this article online at wileyonlinelibrary.com.

evaluate accuracy and reproducibility of PWV assessment based on multislice two-directional in-plane VE MRI, capturing the propagation of the velocity waveform along the aorta centerline in patients and in healthy volunteers.

MATERIALS AND METHODS

Subjects

All patients and healthy volunteers gave informed consent and approval from the local Medical Ethical Committee was obtained. Eighteen patients (15 men and 3 women, mean age ± standard deviation [SD] = 59 ± 10 years) with suspected coronary artery disease and 15 healthy nonsmoking volunteers (eight men and seven women, mean age ± SD = 40 ± 13 years) without a history of cardiac disease were prospectively included. Patients underwent cardiac catheterization with elective coronary angiography on clinical indication and within 2 weeks an MRI examination to acquire PWV based on intraaortic pressure–time curves and VE MRI, respectively. All volunteers underwent an MRI examination with repeated PWV assessment after repositioning. Exclusion criteria were evidence of aortic valve stenosis, aortic coarctation or other forms of congenital heart disease, Marfan's syndrome, or general contraindications to MRI. Data of both cohorts were partially included in a previous study describing validation of PWV assessment with multisite one-directional through-plane VE MRI (22).

MRI Acquisition

MRI was performed using a 1.5T scanner (Philips Intera, release 11 and 12; Philips Medical Systems, Best, the Netherlands) with 33 mT/m amplitude, 100 mT/m/ms slew rate, and 0.33 msec rise time. A five-element cardiac coil placed on the chest was used for signal reception. After acquisition of a series of thoracic survey images which were used for planning purposes, a three-slice volume slab of the aorta in double-oblique sagittal view was acquired, capturing as much of the aortic path length as possible, including the aortic root, the complete aortic arch, and the descending aorta down to the most distal part of the abdominal aorta that could be captured in the 3-cm thick volume slab. The body coil was used for radiofrequency (RF) transmission and signal reception. A steady-state free-precession (SSFP) sequence with free breathing was used (scan parameters: 60% rectangular field-of-view (FOV) 450 × 270 mm^2, 10 mm slice thickness without overlap, echo time [TE] 1.4 msec, repetition time [TR] 2.9 msec, flip angle [α] 50°, acquisition voxel size 2.2 × 1.8 × 10.0 mm^3, number of signal averages (NSA) 1, retrospective-gating with 30 phases reconstructed into one average cardiac cycle with arrhythmia rejection acceptance window of 10% variation). The resulting three-slice volume slab (covering a double-oblique sagittal view of the aorta) was used for planning the VE MRI acquisitions. Aortic PWV was subsequently assessed from through-plane (t.p.) VE MRI and in-plane (i.p.) VE MRI.

First, $PWV_{t.p.}$ was assessed from multisite one-directional through-plane VE MRI based on the transit-time method (described and validated previously (22)). Two VE MRI acquisitions were performed at two locations perpendicular to the aorta. The first acquisition, using the five-element cardiac coil for signal reception, was obtained perpendicular to the ascending aorta at the level of the pulmonary trunk, transecting both the ascending and proximal descending aorta distal to the aortic arch. The second acquisition, using the body coil for signal reception, was obtained at the abdominal aorta ≈10 cm below the diaphragm. Velocity-encoding was performed perpendicular to the acquisition planes. Scan parameters: 90% rectangular FOV 300 × 270 mm^2, 8 mm slice thickness, TE 2.9 msec, TR 4.9 msec, α 20°, acquisition voxel size 2.3 × 2.1 × 8.0 mm^3, sampling bandwidth 449 Hz, NSA 2, retrospective gating with maximal number of phases reconstructed into one average cardiac cycle with arrhythmia rejection window set to acceptance of 15% variation (resulting in an effective temporal resolution of the resulting flow velocity graph of 6–10 msec depending on the heart rate; the true temporal resolution is determined by TR and the VE acquisitions, and amounted to 9.8 msec). The velocity-sensitivity for the first acquisition at the proximal aorta was set to 150 cm/s and for the second acquisition at the abdominal aorta to 100 cm/s. Acquisition was performed with free breathing without respiratory compensation and scan time of a single acquisition was almost 4 minutes at a heart rate of 60 bpm.

Second, $PWV_{i.p.}$ was assessed by means of two consecutive multislice two-directional in-plane VE MRI acquisitions of the three-slice double-oblique sagittal stack of the aorta. In Fig. 1 a schematic representation of $PWV_{i.p.}$ assessment is given. Velocity-encoding was performed in phase-encoding or anterior-posterior (AP) direction and in frequency-encoding or feet-head (FH) direction, respectively, with velocity sensitivity set to 150 cm/s. Scan parameters: 60% rectangular FOV 450 × 270 mm^2, 10 mm slice thickness, TE 2.4 msec, TR 4.3 msec, α 10°, acquisition voxel size 3.5 × 2.1 × 10.0 mm^3, sampling bandwidth 495 Hz, NSA 2, retrospective gating with maximal number of phases reconstructed into one average cardiac cycle with arrhythmia rejection window set to acceptance of 15% variation (resulting in an effective temporal resolution of the resulting flow velocity graph of 6–10 msec depending on the heart rate; the true temporal resolution is determined by TR and VE acquisitions, and amounted to 8.6 msec). Acquisition was performed with free breathing without respiratory compensation and scan time of a single acquisition amounted to 7 minutes 42 seconds at a heart rate of 60 bpm.

Image Processing

$PWV_{t.p.}$ was obtained from the two single-slice acquisitions with one-directional through-plane VE MRI. In the resulting velocity images the cross-sectional blood flow velocities of the ascending, proximal descending, and distal descending aorta were obtained by automated contour detection using the in-house-developed

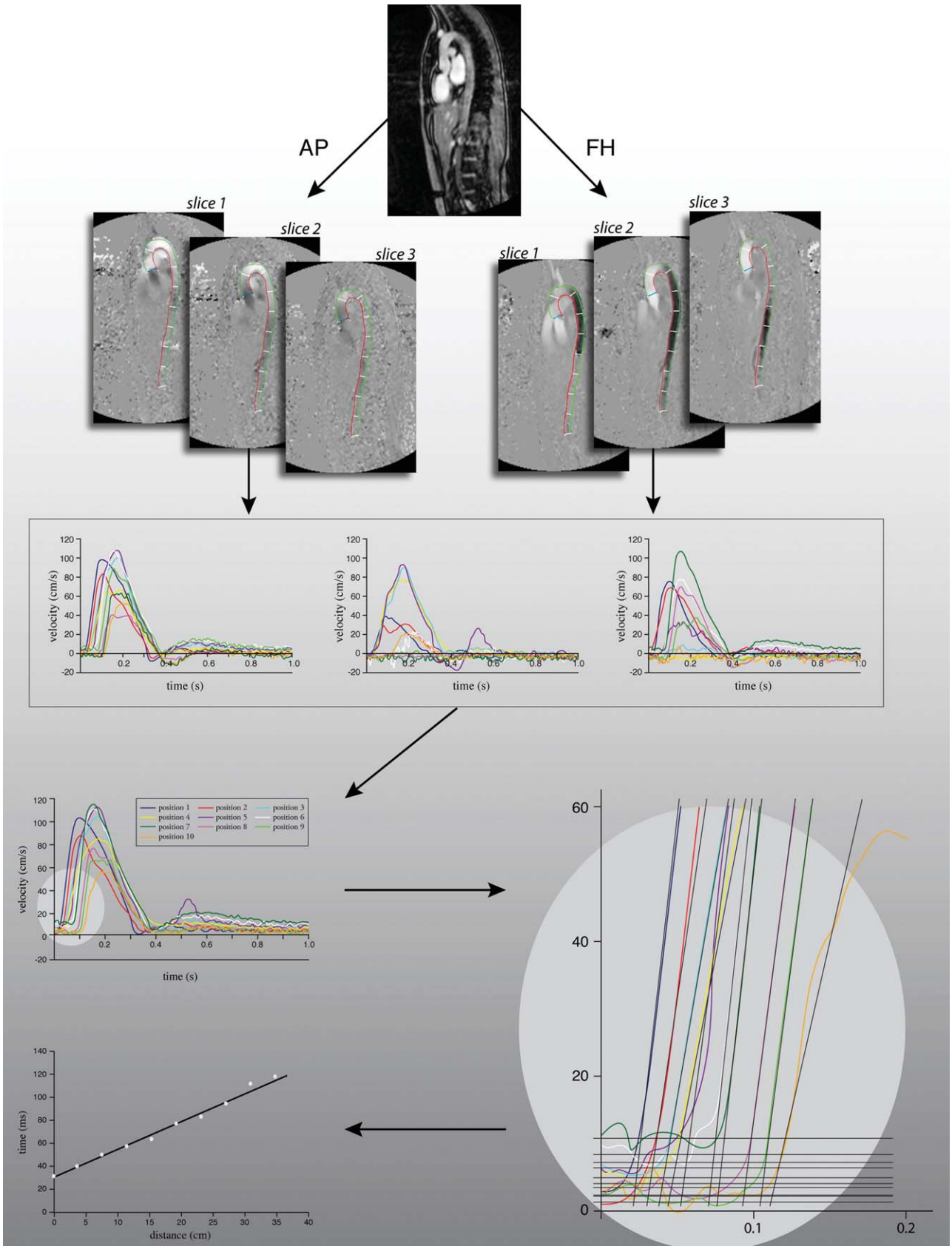

Figure 1. $PWV_{i.p.}$ assessment by multislice two-directional in-plane velocity-encoded MRI. A double-oblique stack of three consecutive slices covering the full aorta is acquired with anterior-posterior and feet-head velocity-encoding (panels second row). Flow velocity waveforms are determined from the maximal velocity detected over the lumen per phase at 200 sample points equidistantly distributed along the centerline of the aorta. For each slice, this results in 200 flow velocity-time graphs (panels third row). For each sample point and each phase, the maximal velocity value over the three slices is determined (ie, maximal velocity projection), resulting in the maximal flow velocity wave form of blood flowing along the aorta (panel fourth row left). The arrival time of each of the 200 wave forms at their corresponding positions along the aortic centerline is automatically determined by the transection of the mean diastolic flow velocity and the upslope of the systolic wave front (panel fifth row right). The arrival times are plotted against the position along the centerline and $PWV_{i.p.}$ between two measurement sites is determined by the inverse of the slope, determined by linear regression of the arrival time-position relation (panel fifth row left). In the velocity graphs, waveforms at only 10 sample locations are presented.

FLOW software package (Leiden University Medical Center, Leiden, the Netherlands) (23). For each of the three aortic measurement sites the mean cross-sectional blood flow velocity for each phase was plotted against time, resulting in three aortic blood flow velocity wave forms. The arrival time of the front of each of these waves was automatically determined from the transsection of the horizontal offset line modeling the mean diastolic flow velocity and a line following the upslope of the systolic flow velocity wave front modeled by linear regression of the flow velocity values between 20% and 80% of the total range of the slope, respectively. $PWV_{t.p.}$ was defined as the ratio between the distance between the individual measurement sites (measured by a poly-line manually traced along the aortic centerline in the double-oblique three-slice sagittal stack of the aorta) and the difference in arrival time (ie, the transit time).

$PWV_{i.p.}$ was obtained from the two three-slice acquisitions with two-directional in-plane VE MRI using the in-house-developed MASS software package (Leiden University Medical Center) (24). First, the aorta was manually segmented with one set of contours that was subsequently copied to all slices, all phases and to both AP and FH encoding series (Fig. 1). Next, the aortic centerline was automatically determined in MASS from the contour set and 200 equidistantly spaced chords perpendicular to the centerline were defined. For each pixel the velocity in the direction parallel along the centerline (perpendicular to the chord) was constructed from the velocity components in AP and FH direction. The aortic flow velocity was sampled along each chord and the maximal velocity per chord was determined. To avoid phase dispersion effects from voxels at the aorta vessel wall boundaries (25,26), only sample points from the inner 50% of each chord were taken into account. For each slice this resulted eventually in 200 flow velocity-time graphs. Next, for each chord and each phase the maximal velocity value over the three slices was determined (ie, maximal velocity projection). For each chord this resulted in the maximal flow velocity wave form of blood flowing along the aorta.

Areas with artifacts present in the velocity images (eg, due to intravoxel dephasing (25,26)) and areas with overlying flow structures potentially obscuring the aortic trajectory in the other slices (such as the pulmonary artery overlying part of the promixal descending aorta), which may corrupt the determination of the maximal aortic flow velocity projection over the three slices, were excluded.

The distance along the aortic centerline was manually traced by a poly-line in the slab of the three sagittal slices. The arrival time of each of the 200 wave forms at their corresponding positions along the aortic centerline was automatically determined similarly as for the $PWV_{t.p.}$ assessment by the determination of the transection point of the mean diastolic flow velocity and the upslope of the systolic wave front. The arrival times were plotted against the position along the centerline and the $PWV_{i.p.}$ between two measurement sites was determined by the inverse of the slope that was determined by linear regression of the arrival time-position relation.

Both $PWV_{t.p.}$ and $PWV_{i.p.}$ of the proximal aorta, distal aorta, and total aorta were determined for all patients and volunteers.

Pressure Measurements

In eighteen patients, invasive pressure-time curves and simultaneous electrocardiogram (ECG) recordings were obtained during cardiac catheterization immediately after vascular access to avoid interference by medication or interventional procedures. Pressure measurements were obtained by a 6F JR4 pressure tip catheter (Cordis, Miami, FL) that was introduced through a 6F sheath (Cordis) into either one of the femoral arteries and advanced through the aorta until just distal to the aortic valve. During pullback the catheter tip was consecutively moved to 8 to 10 locations 5.8 cm apart. At each location, pressure-time curves were recorded with a sampling resolution of 2 kHz during at least 10 cardiac cycles to take into account possible respiration-induced changes in the blood pressure-time curves. The onset of each systolic pressure wave was automatically determined at the time point of minimal pressure, relative to the preceding R-wave. For each location the mean arrival time of the pressure wave was determined and plotted versus the location along the aorta. The $PWV_{pressure}$ was determined by the inverse of the slope that was determined by linear regression of the arrival time-position relation.

Experiments and Statistical Analysis

In patients selected for cardiac catheterization, $PWV_{pressure}$ was determined for the total aorta and subsequently compared with $PWV_{t.p.}$ and $PWV_{i.p.}$ as assessed with MRI. In healthy volunteers, $PWV_{t.p.}$ and $PWV_{i.p.}$ assessments for the proximal, distal, and total aorta were repeated after repositioning of the volunteer in the MRI scanner. Repeated PWV assessment was compared as well as $PWV_{t.p.}$ versus $PWV_{i.p.}$. Data of 10 randomly selected volunteers were analyzed twice by one observer (J.W.) and once by another observer (P.v.d.B.), to test inter- and intraobserver variation. Repeated analyses were performed blinded with respect to previous results. Interexamination time for intraobserver analysis was more than 1 month.

Continuous variables are expressed as mean ± SD. Mean signed differences and the 95% confidence interval (95% CI) were determined for paired variables and the statistical significances of these differences were studied using paired *t*-tests. A significance level $P < 0.05$ was used. The coefficient of variation (COV), defined as the SD of the differences divided by the mean of both measurements, was determined to express the variation between measurements. Bland–Altman plots (27) were determined to study systematic differences. Statistical significance of the difference between correlation coefficients for $PWV_{i.p.}$ and $PWV_{t.p.}$ versus $PWV_{pressure}$ was tested by stepwise regression analysis with PWV from MRI as dependent variable and $PWV_{pressure}$ and the interaction between $PWV_{pressure}$ and in-plane versus through-plane VE MRI as predictors.

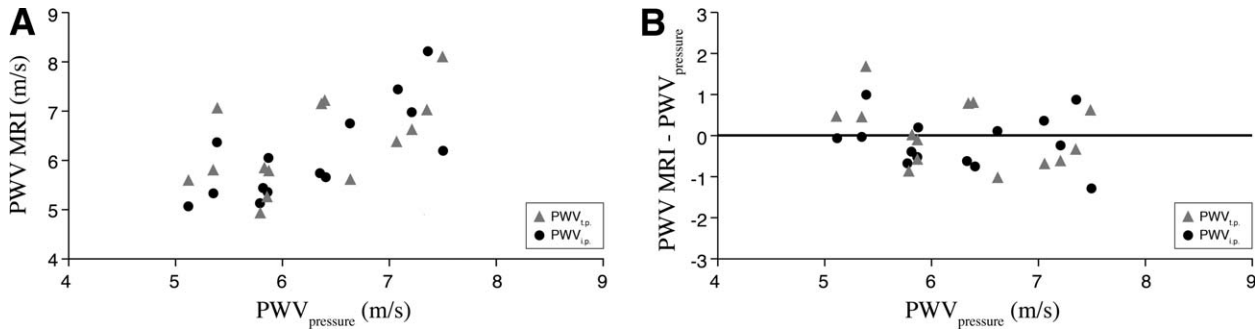

Figure 2. Correlation (A) and Bland–Altman plot **(B)** for MRI-assessed PWV vs. $PWV_{pressure}$ for both through-plane velocity-encoded MRI ($PWV_{t.p.}$) as well as in-plane velocity-encoded MRI ($PWV_{i.p.}$).

A significant interaction indicates significant different correlation.

Correlation, variation between variables as well as the intra- and interobserver agreement was tested by the intraclass correlation coefficient (ICC) for absolute agreement. All statistical analyses were performed using SPSS v. 16.0 (SPSS, Chicago, IL).

RESULTS

For the current study, data were used that were previously published (22), in which 18 patients were included to validate $PWV_{t.p.}$ with $PWV_{pressure}$. From this cohort, four patients were excluded from $PWV_{i.p.}$ validation. The additional scan time needed to acquire the two in-plane VE MRI sequences was too long for these patients to tolerate. In two patients, in-plane VE MRI was not attempted at all and the two other patients moved during acquisition, resulting in unacceptable image quality. In the remaining 14 patients and in all volunteers, assessment of $PWV_{t.p.}$ and $PWV_{i.p.}$ with VE MRI was successfully performed. In the patients, $PWV_{pressure}$ of the total aorta was compared with $PWV_{t.p.}$ and $PWV_{i.p.}$. The results are presented in Fig. 2: correlation between pressure-derived and MRI-derived PWV is presented in Fig. 2A and the differences are presented in the Bland–Altman plot in Fig. 2B. No obvious trend in bias for $PWV_{t.p.}$ or $PWV_{i.p.}$ versus $PWV_{pressure}$ was observed. The statistical results are presented in Table 1. $PWV_{i.p.}$ showed a significantly stronger ($P < 0.001$) correlation with $PWV_{pressure}$ than $PWV_{t.p.}$ (Pearson correlation $r = 0.75$ [$P = 0.002$] vs. $r = 0.58$ [$P = 0.03$], respectively). The variation between $PWV_{pressure}$ and $PWV_{t.p.}$ amounted to 12% and between $PWV_{pressure}$ and $PWV_{i.p.}$ 10%.

In 15 healthy volunteers, $PWV_{t.p.}$ and $PWV_{i.p.}$ were assessed twice with VE MRI, for the proximal, distal, and total aorta. The difference in heart rate during both $PWV_{t.p.}$ assessments was not statistically significant but the heart rate during the second $PWV_{i.p.}$ assessment was on average 2.5 beats/minute higher ($P = 0.04$) than during the first $PWV_{i.p.}$ assessment. The results of the repeated PWV assessments are presented in Fig. 3; Fig. 3A,B presents the correlation and differences of the repeated assessment for $PWV_{t.p.}$ and $PWV_{i.p.}$ for the proximal aorta, Fig. 3C,D for the distal aorta, and Fig. 3E,F for the total aorta. No obvious trends in bias for repeated assessments of $PWV_{t.p.}$ or $PWV_{i.p.}$ were present. The results of the statistical analyses are presented in Table 2. For both the proximal and distal aorta, as well as for the total aorta, repeated assessments of $PWV_{i.p.}$ showed stronger Pearson correlation and less variation ($r = 0.97$ [$P < 0.001$] and COV = 10% for proximal aorta, $r = 0.94$ [$P < 0.001$] and COV = 12% for distal aorta and $r = 0.97$ [$P < 0.001$] and COV = 7% for the total aorta) than repeated $PWV_{t.p.}$ assessment ($r = 0.69$ [$P = 0.005$] and COV = 17% for proximal aorta, $r = 0.90$ [$P < 0.001$] and COV = 16% for distal aorta and $r = 0.90$ [$P < 0.001$] and COV = 13% for the total aorta). Notably, the mean differences in repeated assessments were small but significantly different for $PWV_{i.p.}$ (0.4 m/s for both proximal [$P = 0.03$] and distal aorta [$P = 0.02$], and 0.2 m/s for total aorta [$P = 0.03$], respectively), whereas for $PWV_{t.p.}$ the mean differences were on same order of magnitude (0.4 m/s for proximal aorta, 0.3 m/s for both distal and total aorta, respectively), but due to the larger SD, these differences were not statistically significant. Furthermore, comparing $PWV_{i.p.}$ with $PWV_{t.p.}$ revealed statistically significant differences: a mean difference of $PWV_{i.p.}$ versus $PWV_{t.p.}$ of 0.9 m/s for proximal aorta ($P = 0.002$) and −0.5 m/s for distal aorta ($P = 0.02$).

Results for inter- and intraobserver analyses are presented in Table 3. The differences in PWV between analyses by two observers and between repeated analyses by one observer were small and nonsignificant (only differences for $PWV_{i.p.}$ assessment in the total aorta were statistically significant, but with a mean difference of 0.1 m/s [$P = 0.04$] for intra- and 0.2 m/s

Table 1
$PWV_{pressure}$ versus $PWV_{t.p.}$ and $PWV_{i.p}$

	$PWV_{t.p.}$	$PWV_{i.p.}$
N	14	14
Mean difference ± SD (m/s)	+0.1±0.8	-0.1±0.6
P	0.79	0.43
Pearson *r*	0.58(P=0.03)	0.75(P=0.003)
95%CI (m/s)	-0.4 – 0.5	-0.5 – 0.2
COV (%)	12%	10%

$PWV_{t.p.}$: Pulse Wave Velocity from through-plane velocity-encoded MRI; $PWV_{i.p.}$: Pulse Wave Velocity from in-plane velocity-encoded MRI; SD: standard deviation; 95%CI: 95% confidence interval; COV: coefficient of variation.

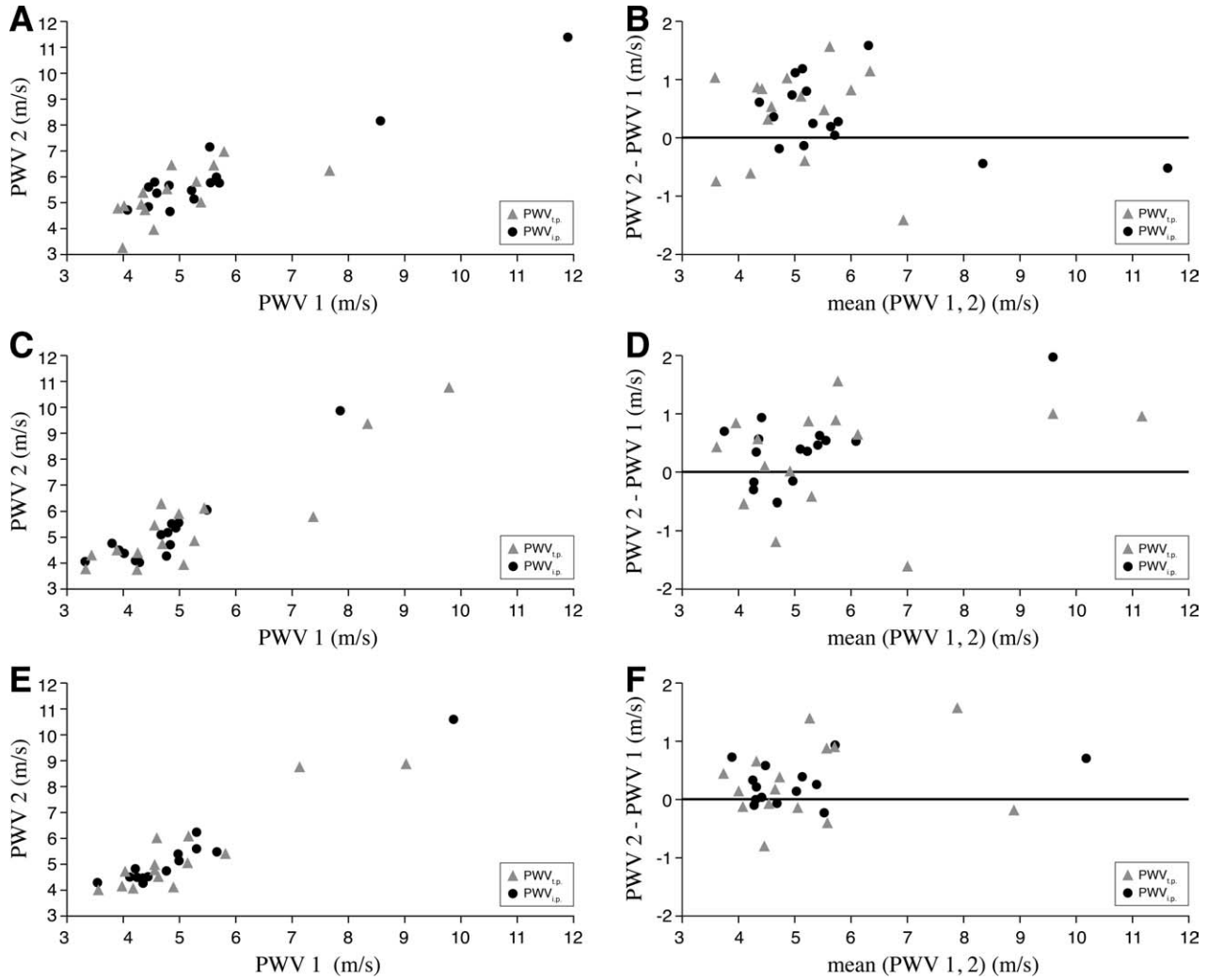

Figure 3. Correlation and Bland–Altman plots for repeated assessment of $PWV_{t.p.}$ and $PWV_{i.p.}$, for the proximal aorta **(A,B)**, distal aorta **(C,D)**, and total aorta **(E,F)**.

[$P = 0.03$] for interobserver analysis, clinically nonsignificant). Intraclass correlation showed excellent agreement for inter- and intraobserver analysis. The ICC values for $PWV_{t.p.}$ were slightly higher than for $PWV_{i.p.}$ (intraobserver ICC = 0.99 in proximal aorta, 1.00 in distal aorta, and 0.98 in total aorta vs. ICC = 0.94, 0.98, and 0.97; interobserver ICC = 0.94, 0.98, and 0.99 vs. ICC = 0.81, 0.92, and 0.95, respectively).

DISCUSSION

The main findings of this study are: 1) Assessment of aortic pulse wave velocity by in-plane VE MRI is significantly different from assessment by through-plane VE MRI (ie, using the conventional transit-time method); 2) PWV by in-plane VE MRI shows higher agreement with values from invasive pressure measurements (ie, gold standard) than PWV by through-plane VE MRI; 3) PWV by in-plane VE MRI shows higher reproducibility than by through-plane VE MRI; 4) Inter- and intraobserver variations in image analysis are small for both MRI methods but variation is slightly higher for in-plane VE MRI.

The compliance of the aortic vessel wall regulates the damping of the blood flow wave that is ejected from the left ventricle during systole and that propagates towards the periphery and the end-organs. In addition, it maintains the blood supply to the heart (ie, the coronary circulation) and other organs during diastole. Numerous reports have used VE MRI to assess the aortic PWV (8,13–15,20–22), almost exclusively using the transit-time method with one-directional through-plane velocity-encoding at multiple sites perpendicular to the aorta. Rogers et al (28), Yu et al. (29), and Fielden et al. (30) assessed PWV from in-plane VE MRI acquisitions. These studies used either one-directional (in frequency-encoding or FH direction) or two-directional (both in phase-encoding or AP direction and in frequency-encoding or FH direction) in-plane velocity-encoding in a single double-oblique sagittal plane of the aorta to obtain the aortic PWV. Adding velocity-encoding in AP direction enables PWV assessment in the aortic arch in contrast to the single one-directional FH velocity-encoding, which is limited to PWV assessment in the ascending and descending aorta only. Also, in order to achieve

Table 2
Repeated $PWV_{t.p.}$ and $PWV_{i.p.}$ assessment

	Proximal aorta			Distal aorta			Total aorta		
	Repeat $PWV_{t.p.}$	Repeat $PWV_{i.p.}$	$PWV_{i.p.}$ vs. $PWV_{t.p.}$	Repeat $PWV_{t.p.}$	Repeat $PWV_{i.p.}$	$PWV_{i.p.}$ vs. $PWV_{t.p.}$	Repeat $PWV_{t.p.}$	Repeat $PWV_{i.p.}$	$PWV_{i.p.}$ vs. $PWV_{t.p.}$
N	15	15	30	15	15	30	15	15	30
Mean difference± SD (m/s)	0.4±0.8	0.4±0.6	0.9±1.4	0.3±0.9	0.4±0.6	-0.5±1.1	0.3±0.7	0.2±0.4	-0.1±0.8
P	0.08	0.03	0.002	0.26	0.02	0.02	0.10	0.03	0.57
Pearson *r*	0.69(P=0.005)	0.97(P<0.001)	0.66(P<0.001)	0.90(P<0.001)	0.94(P<0.001)	0.83(P<0.001)	0.90(P<0.001)	0.97(P<0.001)	0.84(P<0.001)
95% CI (m/s)	-0.0 – 0.8	0.1 – 0.7	0.4 – 1.4	-0.2 – 0.7	0.1 – 0.7	-0.9 – -0.1	-0.0 – 0.6	0.0 – 0.4	-0.4 – 0.2
COV (%)	17%	10%	26%	16%	12%	21%	13%	7%	16%

$PWV_{t.p.}$: Pulse Wave Velocity from through-plane velocity-encoded MRI; $PWV_{i.p.}$: Pulse Wave Velocity from in-plane velocity-encoded MRI; SD: standard deviation; 95%CI: 95% confidence interval; COV: coefficient of variation.

the highest possible temporal resolution in the flow velocity graphs, we used consecutive acquisitions with one-directional in-plane velocity-encoding in the AP and FH directions, respectively, and both acquisitions were combined retrospectively in order to construct the velocity in the direction of the aortic centerline, instead of performing a single acquisition with two-directional in-plane velocity-encoding (29,30) which holds a potentially 33% lower true temporal resolution. Furthermore, our approach using three consecutive slices with maximal velocity projection to determine the maximal aortic velocity propagating along the centerline enables assessment of the aortic flow velocity with more coverage of aortic trajectory in case of a high degree of tortuosity. Fielden et al (30) used a cross-correlation algorithm to obtain the transit-time of the wave front propagation between two sample locations and they showed better reproducibility than when using thresholding (Yu et al (29)) or linear regression (Rogers et al (28) and this study) algorithms for detecting the onset of the systolic wave front. Implementation of a cross-correlation algorithm in the current approach could be a potential improvement regarding reproducibility.

In our study the accuracy and reproducibility of the MRI-assessed PWV by in-plane VE MRI were evaluated by validation against invasive pressure measurements and by comparison of repeated MRI examinations, which was not investigated before. Grotenhuis et al (22) validated the $PWV_{t.p.}$ assessment (where transit-time method was defined on the propagation of the flow wave) with invasive pressure measurements and found a moderate Pearson correlation between $PWV_{t.p.}$ and $PWV_{pressure}$ of 0.53 with small and nonsignificant differences between both techniques. Even though our method defined the transit-time on the propagation of the flow velocity wave, our findings for $PWV_{t.p.}$ assessment were comparable. For the validation of $PWV_{i.p.}$ assessment against $PWV_{pressure}$, we showed substantially higher agreement with the gold standard for $PWV_{i.p.}$ than for $PWV_{t.p.}$. Additionally, Grotenhuis et al reported high reproducibility of $PWV_{t.p.}$ without significant bias in repeated assessment. Our findings confirm these results, but furthermore, our study shows that reproducibility of $PWV_{i.p.}$ is higher than $PWV_{t.p.}$. Notably, the differences in repeated PWV assessment show that a second assessment provided a slightly higher PWV-value than the first, both for $PWV_{i.p.}$ as well as for $PWV_{t.p.}$ and for all trajectories. This mean difference was statistically significant for $PWV_{i.p.}$, but, due to the larger SD, not for $PWV_{t.p.}$, which may illustrate the potentially higher sensitivity of $PWV_{i.p.}$ assessment. The systematically higher PWV in the second examination can possibly be ascribed to an increasing aggravation that the long examination time for repeated scanning induced on the volunteers, which is possibly indicated by the significantly increased heart rate for the second $PWV_{i.p.}$ assessment.

In our methods, $PWV_{i.p.}$ and $PWV_{t.p.}$ utilize different data to detect the onset of the flow velocity wave front (ie, the spatial peak velocity for $PWV_{i.p.}$ and spatial mean velocity for $PWV_{t.p.}$). We assume that this

Table 3
Inter- and Intraobserver Agreement $PWV_{t.p.}$ and $PWV_{i.p.}$ Assessment

		Proximal aorta		Distal aorta		Total aorta	
		$PWV_{t.p.}$	$PWV_{i.p.}$	$PWV_{t.p.}$	$PWV_{i.p.}$	$PWV_{t.p.}$	$PWV_{i.p.}$
Intraobserver	*N*	10	10	10	10	10	10
	Mean difference± SD (m/s)	0.1±0.3	0.1±0.2	0.0±0.1	0.0±0.1	0.1±0.1	0.1±0.2
	P	0.51	0.20	0.30	0.08	0.06	0.04
	ICC (all $P<0.001$)	0.99	0.94	1.00	0.98	0.98	0.97
	95% CI (m/s)	-0.1 – 0.2	-0.0 – 0.2	-0.1 – 0.1	-0.0 – 0.2	0.0 – 0.2	0.0 – 0.2
	COV (%)	6%	4%	2%	3%	3%	3%
Interobserver	*N*	10	10	10	10	10	10
	Mean difference± SD (m/s)	0.1±0.5	0.2±0.4	-0.0±0.3	0.2±0.3	0.1±0.1	0.2±0.2
	P	0.65	0.28	0.62	0.07	0.13	0.03
	ICC (all $P<0.001$)	0.94	0.81	0.98	0.92	0.99	0.95
	95% CI (m/s)	-0.2 – 0.5	-0.1 – 0.4	-0.1 – 0.2	-0.0 – 0.3	-0.0 – 0.2	0.0 – 0.3
	COV (%)	11%	8%	5%	5%	3%	4%</TB

$PWV_{t.p.}$: Pulse Wave Velocity from through-plane velocity-encoded MRI; $PWV_{i.p.}$: Pulse Wave Velocity from in-plane velocity-encoded MRI; SD: standard deviation; ICC: intraclass correlation coefficient; 95%CI: 95% confidence interval; COV: coefficient of variation.

difference will have little effect on the time of the onset of the wave front, which is what is used in the PWV estimations. The spatial mean velocity will be less noise-sensitive but the spatial peak velocity will have a better agreement with $PWV_{i.p.}$ assessment. Image analysis for $PWV_{i.p.}$ assessment demands more manual user interaction than for $PWV_{t.p.}$ assessment. This is also evident from the slightly lower inter- and intraobserver agreement for repeated analyses for $PWV_{i.p.}$ assessment. Still, the agreement was excellent and differences between analyses were small and clinically nonsignificant and can be potentially solved by automated processing methods.

Our study has limitations. No correction for phase offset errors was made (31,32). For the method introduced in our study it is not essential to obtain the true local velocity value, since only the onset of the velocity wave form is detected and used for PWV definition. We assume that a local offset error will have no effect on this algorithm.

Furthermore, due to acquisition time constraints, only in-plane velocity-encoding in two directions was performed in two separate series. The contribution of the through-plane velocity component (ie, right-left direction in the double-oblique sagittal stack) to the velocity wave form propagating along the centerline of the aorta, and in particular the contribution of this component to the detection of the onset of the wave form, was considered to be small. Adding this velocity component to the imaging data is feasible, but at a penalty of 33% more scanning time. The long acquisition time for $PWV_{i.p.}$ assessment is demanding for patients and the total examination time proved to be a limitation in four patients. On the other hand, total MRI examination time was long because both $PWV_{i.p.}$ and $PWV_{t.p.}$ were obtained for this study.

A hardware limitation is the use of the five-element phased-array cardiac receive-coil. The coverage of these elements was not sufficient to perform acquisition in the whole aorta in all subjects, and since no other cardiac coil was available for this study, the body coil was used for acquisition of the in-plane VE MRI and the through-plane VE MRI at the lower level in the aorta. This will result in a degradation of signal-to-noise compared to the through-plane VE MRI at the upper aortic level. The use of a receive-coil with coverage of the abdominal aorta can potentially improve image quality of the through-plane VE MRI in the abdominal aorta and of the in-plane VE MRI acquisitions.

Another limitation is the comparison of MRI-assessed PWV with the gold standard (ie, invasive pressure measurements). The PWV-values assessed with invasive pressure measurements were obtained on average 2 weeks before the MRI examination. As was also evident in the study by Grotenhuis et al (22), the physiological variation of PWV as part of day-to-day differences in blood pressure, blood flow, and sympathic tone may explain the variation and moderate correlation between pressure measurements and MRI-assessed PWV-values.

In conclusion, this study describes aortic PWV assessment based on two-directional in-plane VE MRI. This method is an improvement over the conventional transit-time method for PWV assessment, with a higher agreement with the gold standard and a higher reproducibility. Furthermore, this method provides PWV-values at a regional level in the aorta, which is potentially of high interest in specific cardiovascular diseases with regional manifestation of impaired aortic compliance such as in patients with Marfan's syndrome.

ACKNOWLEDGMENTS

We thank Gerrit Kracht for graphic design and Gerda Labadie for patient and volunteer recruitment.

REFERENCES

1. Ohmori K, Emura S, Takashima T. Risk factors of atherosclerosis and aortic pulse wave velocity. Angiology 2000;51:53–60.
2. Safar ME, Henry O, Meaume S. Aortic pulse wave velocity: an independent marker of cardiovascular risk. Am J Geriatr Cardiol 2002;11:295–298.
3. Sutton-Tyrrell K, Najjar SS, Boudreau RM, et al. Elevated aortic pulse wave velocity, a marker of arterial stiffness, predicts

cardiovascular events in well-functioning older adults. Circulation 2005;111:3384–390.
4. Willum-Hansen T, Staessen JA, Torp-Pedersen C, et al. Prognostic value of aortic pulse wave velocity as index of arterial stiffness in the general population. Circulation 2006;113:664–670.
5. Mitchell GF, Guo CY, Benjamin EJ, et al. Cross-sectional correlates of increased aortic stiffness in the community: the Framingham Heart Study. Circulation 2007;115:2628–2636.
6. Oxlund H, Rasmussen LM, Andreassen TT, Heickendorff L. Increased aortic stiffness in patients with type 1 (insulin-dependent) diabetes mellitus. Diabetologia 1989;32:748–752.
7. Cruickshank K, Riste L, Anderson SG, Wright JS, Dunn G, Gosling RG. Aortic pulse-wave velocity and its relationship to mortality in diabetes and glucose intolerance: an integrated index of vascular function? Circulation 2002;106:2085–2090.
8. van Elderen SGC, Brandts A, Westenberg JJM, et al. Aortic stiffness is associated with cardiac function and cerebral small vessel disease in patients with type 1 diabetes mellitus: assessment by magnetic resonance imaging. Eur Radiol 2010;20:1132–1138.
9. Laurent S, Boutouyrie P, Asmar R, et al. Aortic stiffness is an independent predictor of all-cause and cardiovascular mortality in hypertensive patients. Hypertension 2001;37:1236–1241.
10. Safar ME, Levy BI, Struijker-Boudier H. Current perspectives on arterial stiffness and pulse pressure in hypertension and cardiovascular diseases. Circulation 2003;107:2864–2869.
11. Laurent S, Katsahian S, Fassot C, et al. Aortic stiffness is an independent predictor of fatal stroke in essential hypertension. Stroke 2003;34:1203–1206.
12. McEniery CM, Wilkinson IB, Avolio AP. Age, hypertension and arterial function. Clin Exp Pharmacol Physiol 2007;34:665–671.
13. Brandts A, van Elderen SGC, Westenberg JJM, et al. Association of aortic arch pulse wave velocity with left ventricular mass and lacunar brain infarcts in hypertensive patients: assessment with MR imaging. Radiology 2009;253:681–688.
14. Nollen GJ, Groenink M, Tijssen JP, van der Wall EE, Mulder BJM. Aortic stiffness and diameter predict progressive aortic dilatation in patients with Marfan syndrome. Eur Heart J 2004;25: 1146–1152.
15. Groenink M, Lohuis TA, Tijssen JG, et al. Survival and complication free survival in Marfan's syndrome: implications of current guidelines. Heart 1999;82:499–504.
16. Lehmann ED. Clinical value of aortic pulse-wave velocity measurement. Lancet 1999;354:528–529.
17. Lehmann ED. Aortic pulse-wave velocity versus pulse pressure and pulse-wave analysis. Lancet 2000;355:412.
18. Tillin T, Chambers J, Malik I, et al. Measurement of pulse wave velocity: site matters. J Hypertens 2007;25:383–389.
19. Laurent S, Cockcroft J, Van Bortel L, et al. Expert consensus document on arterial stiffness: methodological issues and clinical applications. Eur Heart J 2006;27:2588–2605.
20. Boese JM, Bock M, Schoenberg SO, Schad LR. Estimation of aortic compliance using magnetic resonance pulse wave velocity measurement. Phys Med Biol 2000;45:1703–1713.
21. Vulliémoz S, Stergiopulos N, Meuli R. Estimation of local aortic elastic properties with MRI. Magn Reson Med 2002;47:649–654.
22. Grotenhuis HB, Westenberg JJM, Steendijk P, et al. Validation and reproducibility of aortic pulse wave velocity as assessed with velocity-encoded MRI. J Magn Reson Imaging 2009;30:521–526.
23. van der Geest RJ, Niezen RA, van der Wall EE, de Roos A, Reiber JHC. Automated measurement of volume flow in the ascending aorta using MR velocity maps: evaluation of inter- and intraobserver variability in healthy volunteers. J Comput Assist Tomogr 1998;22:904–911.
24. van der Geest RJ, de Roos A, van der Wall EE, Reiber JHC. Quantitative analysis of cardiovascular MR images. Int J Card Imaging 1997;13:247–258.
25. Hamilton CA. Correction of partial volume inaccuracies in quantitative phase contrast MR angiography. Magn Reson Imaging 1994;12:1127–1130.
26. Tang C, Blatter DD, Parker DL. Accuracy of phase-contrast flow measurements in the presence of partial-volume effects. J Magn Reson Imaging 1993;3:377–385.
27. Bland JM, Altman DG. Statistical methods for assessing agreement between two methods of clinical measurement. Lancet 1986;1:307–310.
28. Rogers WJ, Hu YL, Coast D, et al. Age-associated changes in regional aortic pulse wave velocity. J Am Coll Cardiol 2001;38: 1123–1129.
29. Yu HY, Peng HH, Wang JL, Wen CY, Tseng WY. Quantification of the pulse wave velocity of the descending aorta using axial velocity profiles from phase-contrast magnetic resonance imaging. Magn Reson Med 2006;56:876–883.
30. Fielden SW, Fornwalt BK, Jerosch-Herold M, Eisner RL, Stillman AE, Oshinski JN. A new method for the determination of aortic pulse wave velocity using cross-correlation on 2D PCMR velocity data. J Magn Reson Imaging 2008;27:1382–1387.
31. Gatehouse PD, Rolf MP, Graves MJ, et al. Flow measurement by cardiovascular magnetic resonance: a multi-centre multi-vendor study of background phase offset errors that can compromise the accuracy of derived regurgitant or shunt flow measurements. J Cardiovasc Magn Reson 2010;12:5.
32. Chernobelsky A, Shubayev O, Comeau CR, Wolff SD. Baseline correction of phase contrast images improves quantification of blood flow in the great vessels. J Cardiovasc Magn Reson 2007;9:681–685.